CrystEngComm

PAPER

View Article Online
View Journal

Cite this: DOI: 10.1039/c8ce00798e

The thermo-responsive behavior in molecular crystals of naphthalene diimides and their 3D printed thermochromic composites†

Madushani Dharmarwardana, ‡[a] Bhargav S. Arimilli,‡[a] Michael A. Luzuriaga, [a] Sunah Kwon,[b] Hamilton Lee, [a] Gayan A. Appuhamillage,[a] Gregory T. McCandless,[a] Ronald A. Smaldone *[a] and Jeremiah J. Gassensmith *[ac]

Received 15th May 2018,
Accepted 3rd August 2018

DOI: 10.1039/c8ce00798e

rsc.li/crystengcomm

Herein, we communicate that altering the number of carbon atoms on the alkoxyphenyl substituent in naphthalene diimides results in tunable thermo-salient behavior across a variety of temperatures. Additionally, these compounds were found to display reversible thermochromic behavior in the single crystalline state. We analyzed this behavior using differential scanning calorimetry (DSC), single crystal X-ray diffraction (SXRD), powder XRD (PXRD), and hot-stage microscopy. The heptoxyphenyl-, octoxyphenyl-, and nonoxyphenyl-derivatives exhibited "acrobatic" behavior—namely, bending, jumping, and splitting—upon an irreversible phase transition. This study contributes to a developing paradigm in the understanding of certain naphthalene diimide single crystals that the energy associated with irreversible phase transitions has the potential to perform mechanical work, and that the temperature at which this energy can be fine-tuned by selecting an appropriate alkoxyphenyl substituent. Furthermore, we show that these thermochromic NDI derivatives can be incorporated into commercially-available, polymeric 3D printing materials and the resulting printed mixed polymer-crystalline objects still exhibit thermochromic behavior after incorporation.

Introduction

Tunable thermo-responsive behavior is an area of considerable research interest as these materials can be used potentially in the design of temperature sensors and mechanical actuators. Two of the most common thermo-responsive materials are thermo-mechanically responsive and thermochromic materials and among these two classes, mechanically responsive materials have gained much attention as they have potential applications in sensors, actuators, artificial muscles, and soft robots.[1–3] Polymers that exhibit mechanical motion upon exposure to external stimuli are very common.[3–5] These easily-fabricated materials have been shown to exhibit favorable elastic properties and high degrees of reversibility.[5,6] Mechanically responsive single crystals, however, have potential advantages relative to polymeric materials as they can rapidly convert energy owing to the former's highly ordered periodic structure.[7] Recently, several studies on photo-mechanically responsive molecular crystals have appeared in literature.[1,8–14] To date, only a handful of thermo-mechanically responsive—also known as thermo-salient—organic single crystals have been reported.[7,14–24] These thermo-salient materials can be utilized as fuses,[25] switches, and sensors; however, thermo-mechanical behavior in molecular single crystals and the mechanism behind this motion are still areas of active research with few comprehensive structure–function studies.

Another type of thermo-responsive behavior of interest is thermochromism, which refers to a change in color in response to a change in temperature.[26,27] Thermochromic materials have potential commercial applications as they can be fabricated into temperature sensors.[28] Most thermochromic compounds exhibit positive thermochromism, in which the material's high-temperature phase absorbs energy at a higher wavelength in comparison to its low-temperature phase.[37] The opposite of this phenomenon is negative- or inverse-thermochromism, in which the high-temperature phase absorbs energy at a lower wavelength than the low-temperature phase.[37] Compounds exhibiting inverse thermochromism are rare and have not been extensively reported in literature.[27,29–41] Organic single crystalline thermochromic

[a] Department of Chemistry and Biochemistry, University of Texas at Dallas, 800 West Campbell Road, Richardson, TX 75080-3021, USA.
E-mail: gassensmith@utdallas.edu, ronald.smaldone@utdallas.edu
[b] Department of Material Science and Engineering, University of Texas at Dallas, 800 West Campbell Road, Richardson, TX 75080-3021, USA
[c] Department of Biomedical Engineering, University of Texas at Dallas, 800 West Campbell Road, Richardson, TX 75080-3021, USA

† Electronic supplementary information (ESI) available: Experimental details, single crystal X-ray data, powder X-ray data, NMR spectra, FTIR spectra, and Movie S1–S3. CCDC numbers are 1839983, 1839985–1839987 and 1857158–1857163. For ESI and crystallographic data in CIF or other electronic format see DOI: 10.1039/c8ce00798e

‡ These authors contributed equally to this manuscript.

materials are particularly interesting, but are uncommon. In addition, efforts have been taken to expand the applicability of thermochromic materials in industrial settings. One such effort is the incorporation of thermochromic solids to polymeric matrices to fabricate thin films,[42–44] which has been done for many years. More advanced and contemporaneous methods of fabrication have come into vogue—in particular, additive manufacturing or 3D printing—a method to fabricate specific shapes by adding material in a layer-by-layer fashion using CAD software.[45] 3D printing has become a major industry that is in search of materials and methods for integrating new and existing chemistry.[46–48]

We recently reported[49] that a butoxyphenyl *N*-substituted derivative (BNDI) of naphthalene diimides—a class[50,51] of highly electron-deficient aromatic compounds—exhibits thermo-mechanical properties followed by thermochromism. Thermo-mechanical properties of BNDI were found to be derived from an irreversible phase transition of a non-thermochromic monoclinic polymorph (BNDI-M) to a thermochromic triclinic polymorph (BNDI-T). Upon heating, the BNDI crystals underwent a complete rearrangement of the constituent molecules, releasing the accumulated stress in the form of mechanical motion which was sufficiently powerful to lift a metal ball ~100 times the mass of the crystal itself. We showed that a majority of BNDI crystals became bent during this irreversible phase transition. However, the temperature at which this transition occurs was quite high, restricting the self-actuating behavior to only high-temperature sensing applications. Further, our study left open the possibility that BNDI was unique in its behavior. We wondered whether other derivatives in this family would also actuate and if they would do so at lower-transition temperatures, making them useful in lower-temperature sensing applications.

To investigate this question, we synthesized a library of alkoxyphenyl *N*-substituted NDIs (ANDIs) by modifying the alkane chain emanating from the phenol group. Specifically, we synthesized pentyl- (PNDI), hexyl- (HxNDI), heptyl- (HNDI), octyl- (ONDI), and nonyl- (NNDI) derivatives. After extensive crystallographic, thermal, and optical analysis of ANDI single crystals, it is clear that the majority of ANDIs exhibit thermo-mechanical and thermochromic behavior. To the best of our knowledge, the majority of thermo-responsive molecular crystals only exhibit single-responsive behavior—that is, exhibiting either thermo-mechanical or thermochromic behavior, but not both. Dual responsive behavior—in other words, exhibiting both thermo-mechanical and thermochromic behavior in a single system—is extremely rare.[21] Furthermore, we show that the changes in alkyl chain length on the ANDI molecules alter—but do not eliminate—the thermo-mechanical response of the bulk molecular crystals. Consequently, ANDIs appear to be the first true "family" of thermochromic/thermally-actuating crystals reported. Finally, thermochromic ANDI derivatives exhibit reversible thermochromism in the solid state and have proven to be extremely robust at ambient conditions. Thus, this emerging class of thermochromic single crystals can be appropriated into thermally sensing materials. To demonstrate this concept, we were easily able to incorporate the non-thermosalient crystals of the inversely thermochromic BNDI-T and positively thermochromic HxNDI derivatives into the thermoplastic polylactic acid (PLA) and hot extrude these mixtures into a filament. We then 3D printed different objects using these filaments *via* fused deposition modeling (FDM). These 3D printed objects then exhibited the reversible thermochromic properties of the parent crystals.

Results and discussion

Synthesis and crystallization of ANDI derivatives

All NDI derivatives used in this study were synthesized using naphthalene tetracarboxylic acid dianhydride (NDA). NDA was initially combined with 4-aminophenol to obtain phenyl *N*-substituted NDI (NDI-Ph). This compound was then subjected to nucleophilic substitution of different bromoalkanes to yield a library of ANDI derivatives (Scheme 1).[52] In our previous study, we discovered that BNDI can be crystallized into two stable polymorphs—a thermochromic triclinic phase and a mechanically responsive monoclinic phase.[49] When we tried these same methods to generate single crystal polymorphs for each ANDI derivative, we found that none of them produced high-quality single crystals suitable for single crystal X-ray diffraction (SXRD) analysis.

To grow single crystals, we used our automated flash chromatography system to create gradients of solvent concentrations for each sample. Following chromatographic separation of the crude ANDI derivatives, the resulting solutions sat undisturbed until fully evaporated and each vial was scanned for suitable single crystals. All the ANDI derivatives we report in this manuscript yielded single crystals using this modified slow evaporation technique and we were able to collect SXRD data for each derivative (Table 1). While we were able to obtain single crystals for the PNDI compound, the dataset was low-resolution and the refined and converged structure still had high *R*-factors. Consequently, we omit this system from the crystallographic discussion, but we elaborate upon it in the thermally responsive sections.

Thermo-mechanical and thermochromic behavior of ANDI family

As demonstrated in our previous work, BNDI's irreversible phase transition was found to be associated with the presence of thermo-salient behavior. Thermo-salient behavior

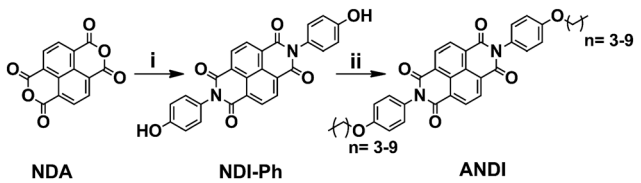

Scheme 1 Synthesis of alkoxyphenyl *N*-substituted naphthalene diimides discussed in this study. (i) 4-Aminophenol, 24 h in DMF. (ii) 1-Bromoalkane of appropriate chain length, 24 h DMF 140 °C.

Table 1 Crystallographic parameters for ANDI derivatives

	BNDI-M	BNDI-T	HxNDI	HNDI	ONDI	NNDI
Temperature/K	100	100	100	100	100	100
Crystal system	Monoclinic	Triclinic	Triclinic	Monoclinic	Triclinic	Monoclinic
Space group	$P2_1/c$	$P\bar{1}$	$P\bar{1}$	$P2_1/n$	$P\bar{1}$	$P2_1/n$
Unit cell/Å a =	5.026(2)	4.1636(8)	8.395(3)	4.1696(15)	4.1680(14)	4.154(2)
b =	33.756(5)	8.1371(18)	8.853(3)	46.595(14)	8.217(3)	51.72(2)
c =	7.9533(14)	20.104(5)	23.938(9)	8.214(3)	24.901(7)	8.253(3)
α =	90°	100.182(11)°	89.528(11)°	90°	97.81(1)°	90°
β =	99.997(10)°	93.124(14)°	80.712(14)°	93.529(10)°	93.453(7)°	93.663(12)°
γ =	90°	94.102(14)°	62.60(2)°	90°	93.834(6)°	90°
Volume/Å^3	1328.8(6)	667.1(3)	1554.3(10)	1592.7(9)	841.0(5)	1769.6(14)
Crystal color	Yellow	Red/orange	Orange	Orange	Orange	Orange
Z	2	1	2	2	1	2
Crystal size/mm	0.84 × 0.14 × 0.10	0.26 × 0.08 × 0.06	0.42 × 0.16 × 0.08	0.24 × 0.08 × 0.06	0.26 × 0.16 × 0.04	0.30 × 0.06 × 0.04
Reflections collected	16 317	14 793	20 000	40 965	20 306	36 862
R_{int}	0.045	0.034	0.044	0.060	0.076	0.095
Calculated density/mg m^{-3}	1.406	1.400	1.322	1.349	1.332	1.319
μ (mm^{-1})	0.10	0.097	0.09	0.09	0.09	0.09
$R[F^2 > 2\sigma(F^2)]$	0.050	0.045	0.055	0.046	0.054	0.055
w$R(F^2)$	0.138	0.115	0.133	0.104	0.120	0.118
Interplanar distance(s)/Å	3.344	3.369	3.413 3.189	3.392	3.402	3.403

includes jumping, splitting, coiling, or other motions in response to heat. So far, the only ANDI derivative this behavior has been observed in is BNDI-M.[49] We thus decided to investigate whether other ANDI derivatives possessing irreversible phase transitions would exhibit the same behavior. The thermo-salient behavior of ANDIs was characterized by DSC, SXRD, and hot-stage microscopy. We first conducted DSC for all derivatives within a temperature range of 25 °C to 240 °C. As shown in Fig. 1, all the compounds undergo phase transitions within this temperature range; however, we have found that the thermo-salient properties occur only during the irreversible phase transitions, which is our primary focus as any thermo-responsive behavior at temperatures higher than 200 °C cannot be analyzed due to operational constraints of our hot-stage microscope.

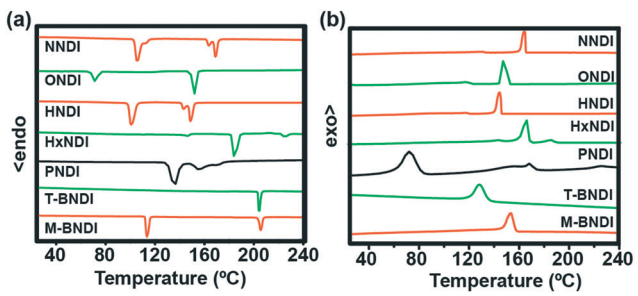

Fig. 1 (a) Heating curves of ANDI derivatives and their corresponding (b) cooling curves. Orange lines correspond to monoclinic crystal systems and green lines correspond to triclinic crystal systems.

DSC analysis of each derivative yielded surprising results and showed that thermo-responsive behaviour in ANDI derivatives is dependent on its alkoxyphenyl substituent and its solid-state packing. As shown in Fig. 1a and S26–S28† and Table 2, compounds BNDI-M, HNDI, ONDI, and NNDI each undergo an irreversible phase transition followed by a reversible phase transition at an even higher temperature. The temperature at which the irreversible phase transition occurs for three derivatives—BNDI-M (4 carbons, 113.46 °C), HNDI (7 carbons, 105.90 °C), and NNDI (9 carbons, 100.69 °C)—decreases as the chain length of the alkane group increases. This similarity in thermal behaviour can also be explained *via* SXRD analysis of BNDI-M, HNDI and NNDI. All three derivatives show similar, herringbone molecular packing and belong to the monoclinic crystal system (Table 1 and Fig. 2). Curiously, ONDI exhibits a lower transition temperature (8 carbons, 72.09 °C) compared to these three derivatives.

Table 2 Summary of properties of ANDI derivatives studied in this manuscript

n	Material	Crystal system	Thermochromic	Thermo-salient	Molecular arrangement	Irreversible phase transition/°C
3	BNDI-M	Monoclinic	✗	✓	Herringbone	113.46
3	BNDI-T	Triclinic	✓	✗	Infinite 1D chains	NA
4	PNDI	NA	✓	✗	NA	NA
5	HxNDI	Triclinic	✓	✗	Infinite 1D chains	NA
6	HNDI	Monoclinic	✓	✓	Herringbone	105.90
7	ONDI	Triclinic	✓	✓	Lamellar	72.09
8	NNDI	Monoclinic	✓	✓	Herringbone	100.69

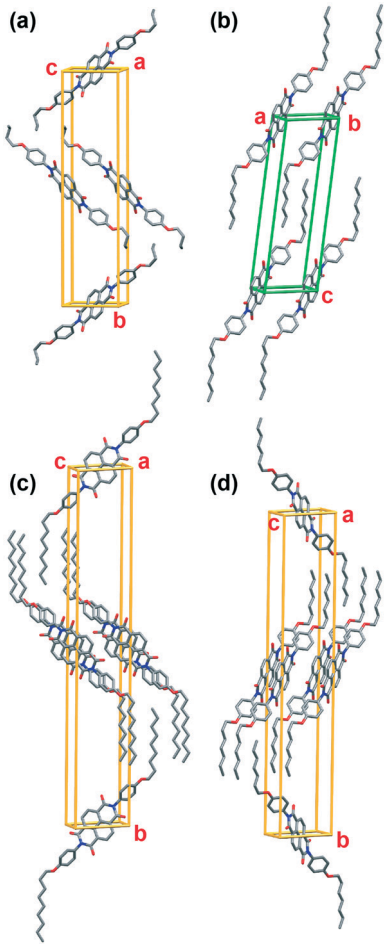

Fig. 2 Comparison of thermo-salient derivative unit cells: (a) BNDI-M (b) ONDI and (c) NNDI (d) HNDI. Orange unit cell axes correspond to monoclinic crystal systems and green unit cell axes correspond to triclinic crystal systems.

Unlike the previous three derivatives, ONDI was solved as a triclinic crystal system and its packing is also slightly different, as it packs in a lamellar array instead of a herringbone arrangement. HxNDI exhibited no irreversible phase transitions and its packing, which is significantly different than the other derivatives, will be discussed later. Finally, PNDI crystals diffracted poorly, limiting SXRD data analysis. However, according to our thermal analysis of PNDI, no irreversible phase transitions were observed (black line, Fig. 1).

We characterized the thermo-responsive behavior of the ANDI single crystals using hot-stage microscopy and SXRD. We first placed each derivative on a polarized optical microscope (POM) heating stage that was cooled under cold nitrogen gas to 0 °C. The samples were then heated, during which we observed thermo-mechanical motion at temperatures beyond the phase transition (Fig. 3).

As shown in Fig. 3a, HNDI single crystals exhibited reversible thermochromism until they reached 105.90 °C. At this temperature, a wave front began at one end of the crystal and moved to the other end, followed by a change in color from orange/yellow to bright yellow (Fig. 3a, Movie S1†). At this

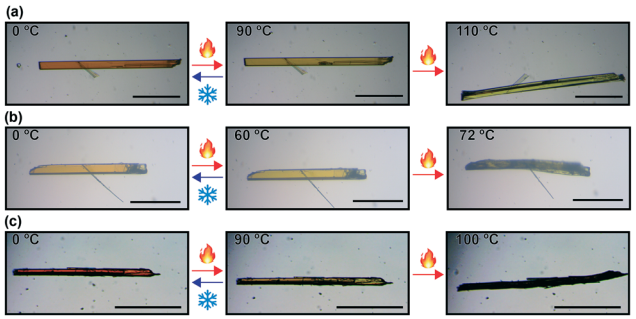

Fig. 3 Thermochromic and thermo-mechanical properties of (a) HNDI, (b) ONDI, and (c) NNDI. First two images in a sequence show thermochromic behaviour (if any) and the final, irreversible step shows the product of the thermo-salient behaviour—typically the crystal splits. Scale bar is 500 μm.

point, crystals began to exhibit motions including bending, jumping, and splitting. After this irreversible phase transition, HNDI crystals were no longer thermochromic and were not suitable for SXRD analysis, as they were no longer single crystalline in nature. Thus, we performed variable temperature PXRD analysis to confirm that the phase transition occurred fully (Fig. S21–S23†).

Similarly, we conducted hot-stage microscopy for NNDI and ONDI, which exhibited similar thermochromic and thermo-mechanical behavior as HNDI (Fig. 3b and c, Movie S2–S4†). Finally, we analyzed the thermo-responsive behavior of HxNDI using hot stage microscopy. As shown in Fig. 4c, we found that HxNDI crystals showed anomalous expansion during heating, with a slight change in the crystal color. However, the crystals returned back to their original size and

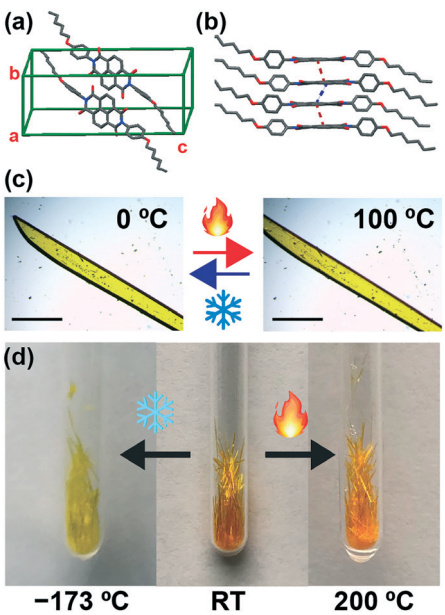

Fig. 4 (a) Unit cell packing structure of HxNDI, (b) alternating interplanar distances of HxNDI (c) POM images showing HxNDI single crystal expansion during heating from 0 °C to 100 °C (scale bar is 500 μm), and (d) thermochromic behaviour of HxNDI.

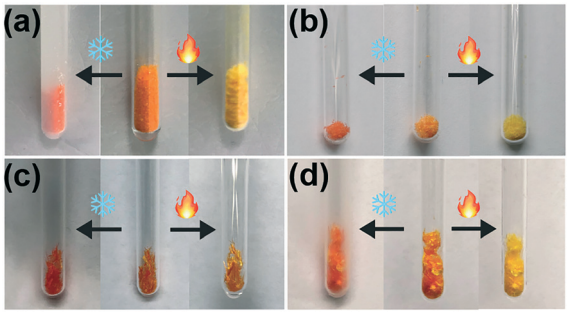

Fig. 5 Thermochromic behavior of (a) PNDI, (b) HNDI, (c) ONDI, and (d) NNDI. All the samples were heated to 100 °C and cooled to −173 °C for the visualization of thermochromic behavior.

color as we cooled the crystals back to room temperature. More importantly, we did not observe any thermo-salient behavior.

In contrast to thermo-salience, we observed that all derivatives studied in this manuscript exhibited some type of thermochromism. Typically, crystals showed red/orange (low temperature) to yellow (high temperature) inverse thermochromic behavior, with the exception of HxNDI, which exhibited yellow (low temperature) to orange (high temperature) positive thermochromic behavior (Table 2, Fig. 5, 4d and S33†). Of all the compounds we analysed in this study, HxNDI exhibited anomalous behavior in the solid state. After careful analysis of its crystal structure, we found that the dihedral angles of HxNDI's two phenyl rings with respect to its NDI core were not the same and measured 55.25(6)° and 74.18(5)°. In contrast, the other ANDI derivatives are symmetric at both ends and thus have matching dihedral angles. Furthermore, BNDI, HNDI, and NNDI each possessed a single interplanar π–π stacking distance (Fig. S10†). HxNDI, however, possessed two interplanar π–π stacking distances—3.413 Å and 3.189 Å—that alternated throughout its crystal structure (Fig. 4b).

Finally, we were able to collect single crystal data of the HNDI, ONDI, and NNDI compounds at 100, 200, and 298 K in an effort to suss out the mechanism of thermochromism (Tables S1–S3†). While more detailed modelling studies are necessary, it is clear that the thermochromism is not a result of changes in bonding; rather, we tentatively attribute these changes to the distance and geometry of adjacent NDI π faces. With that said, additional studies are underway.

3D printing with BNDI-T and HxNDI

The robustness and practical temperature range of the thermochromism of these samples inspired us to attempt to integrate them into thermoplastic matrices to produce thermally responsive polymers. Thermochromic materials have long been used as a visual indicator of surface temperature. With the emergence of 3D printing using thermoplastics, new technologies that can exploit the robust nature of solid-state materials would be a benefit. Since we have identified both positive and negative thermochromic materials, we decided to see if we could make 3D printed composites of each.

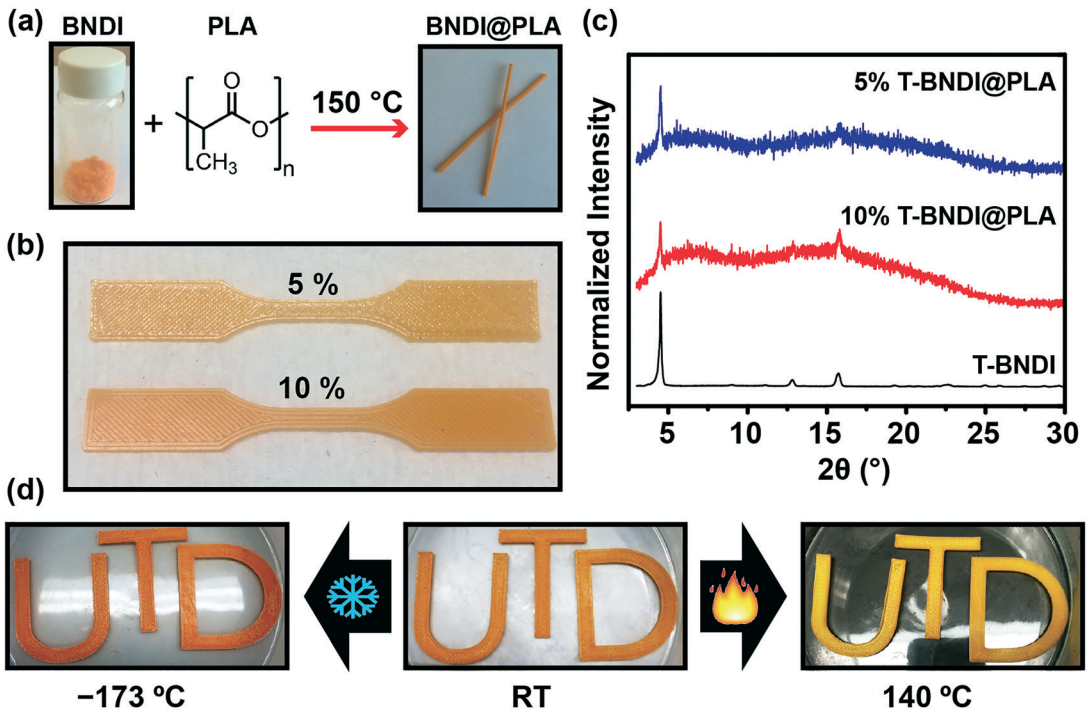

Fig. 6 (a) Schematic diagram of the fabrication of BNDI-T@PLA filaments, (b) varying ratios of BNDI-T incorporated into PLA, (c) PXRD data for BNDI-T@PLA composites, and (d) negative thermochromic behavior of BNDI-T@PLA.

Mixtures of PLA beads—an inexpensive, biodegradable polymeric material commonly used in 3D printing—and crystals of either BNDI-T or HxNDI were added to a filament extruder, which produced long, single wires of ANDI@PLA. We first melted PLA with BNDI-T in 1 : 19 and 1 : 9 ratios at 200 °C (Fig. 6b). The BNDI-T@PLA composite was characterized using PXRD (Fig. 6c). This result demonstrates that the crystalline morphology of BNDI-T does not undergo degradation when incorporated into PLA at elevated temperatures and the resulting plastics appear smooth and the color homogenously distributed. We then tested the thermochromic properties of the BNDI-T@PLA composite. As shown in Fig. 6d, the composite exhibited clear reversible thermochromic behavior. Higher concentrations of BNDI-T showed a more pronounced color change (Fig. 6d).

To visualize positive thermochromism in a polymeric system, HxNDI single crystals were combined with PLA in a 1 : 9 ratio. As seen in Fig. 7, a 3D printed PLA dog bone featuring HxNDI did exhibit modest positive thermochromic behavior, with the low-temperature plastic appearing bright yellow and the high-temperature plastic appearing orange. Again, the 3D printing and hot extrusion did not appear to degrade the crystals inside the filament.

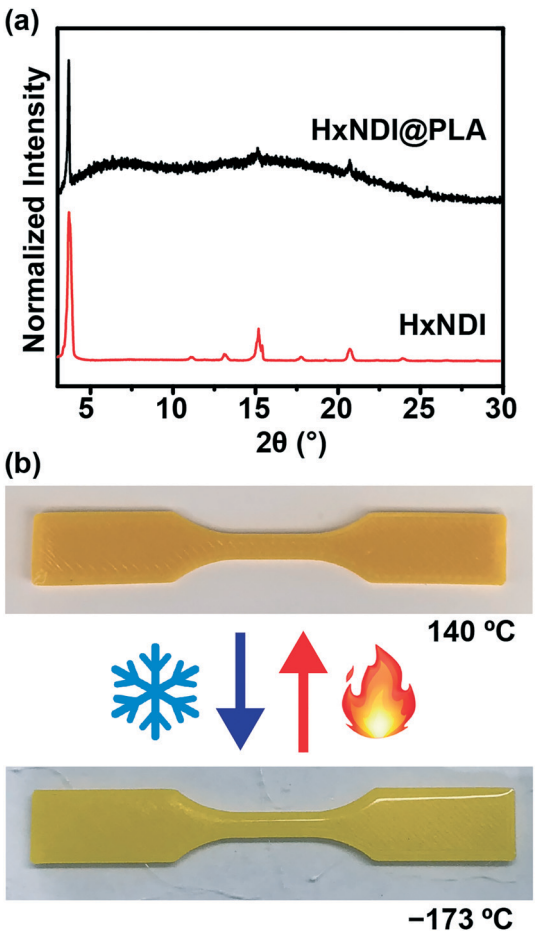

Fig. 7 (a) PXRD data for HxNDI@PLA composites and (b) positive thermochromic behavior of HxNDI @PLA.

Conclusions

We have shown thermally-induced, irreversible phase transitions are a common property of alkoxyphenyl *N*-substituted naphthalene diimides. Some of these single crystals exhibit thermo-salient behavior, such as bending, jumping, and splitting. The temperature at which this behavior occurs can be modulated based on the length of the alkoxyphenyl chain, as observed in our family of derivatives. In general, the temperatures at which thermo-salience occurs decrease with increasing alkyl chain length. In all cases, compounds exhibited thermochromic behavior and this behavior could be reproduced with the 6- and 4-carbon chained ANDI derivatives inside a 3D printed polymeric matrix. Negatively and positively thermochromic 3D printed composites were created using BNDI-T and HxNDI, respectively. With the emergence of 3D printing, temperature-responsive organic single crystals may serve as dopants with organic thermo-polymeric filaments to enhance their use and utility. Finally, it should be mentioned that alkoxyphenyl NDI derivatives have been used in organic electronics as n-type semiconducting materials.[53,54] Even when combined in polymeric systems, it is quite clear a color change (and presumably a band-gap change) occurs based on temperature.

Conflicts of interest

There are no conflicts to declare.

Acknowledgements

We would like to thank Prof. M. C. Biewer for assistance with collecting hot stage polarized optical microscopy data. J. J. G. would like to acknowledge the ACS-PRF (57627-DNI10) and National Science foundation (DMR-1654405) for funding. R. A. S. acknowledges the Department of Energy's National Nuclear Security Agency managed by Honeywell FMT (N000263171) for funding.

References

1 P. Naumov, S. Chizhik, M. K. Panda, N. K. Nath and E. Boldyreva, *Chem. Rev.*, 2015, **115**, 12440–12490.
2 M. Yamada, M. Kondo, J. Mamiya, Y. Yu, M. Kinoshita, C. J. Barrett and T. Ikeda, *Angew. Chem., Int. Ed.*, 2008, **47**, 4986–4988.
3 T. J. White, N. V. Tabiryan, S. V. Serak, U. A. Hrozhyk, V. P. Tondiglia, H. Koerner, R. A. Vaia and T. J. Bunning, *Soft Matter*, 2008, **4**, 1796.
4 A. Natansohn and P. Rochon, *Chem. Rev.*, 2002, **102**, 4139–4176.
5 Y. Yu, M. Nakano and T. Ikeda, *Nature*, 2003, **425**, 145.
6 R. Pelrine, R. Kornbluh, Q. Pei and J. Joseph, *Science*, 2000, **287**, 836–839.
7 N. K. Nath, M. K. Panda, S. C. Sahoo and P. Naumov, *CrystEngComm*, 2014, **16**, 1850.
8 G. R. Krishna, R. Devarapalli, G. Lal and C. M. Reddy, *J. Am. Chem. Soc.*, 2016, **138**, 13561–13567.

9 S. Kobatake, S. Takami, H. Muto, T. Ishikawa and M. Irie, *Nature*, 2007, **446**, 778–781.
10 D. Kitagawa, H. Tsujioka, F. Tong, X. Dong, C. J. Bardeen and S. Kobatake, *J. Am. Chem. Soc.*, 2018, **140**, 4208–4212.
11 D. Kitagawa, K. Kawasaki, R. Tanaka and S. Kobatake, *Chem. Mater.*, 2017, **29**, 7524–7532.
12 A. Takanabe, M. Tanaka, K. Johmoto, H. Uekusa, T. Mori, H. Koshima and T. Asahi, *J. Am. Chem. Soc.*, 2016, **138**, 15066–15077.
13 R. Medishetty, S. C. Sahoo, C. E. Mulijanto, P. Naumov and J. J. Vittal, *Chem. Mater.*, 2015, **27**, 1821–1829.
14 S. Chandra Sahoo, N. K. Nath, L. Zhang, M. H. Semreen, T. H. Al-Tel and P. Naumov, *RSC Adv.*, 2014, **4**, 7640.
15 P. Commins, I. T. Desta, D. P. Karothu, M. K. Panda and P. Naumov, *Chem. Commun.*, 2016, **52**, 13941–13954.
16 Z. Skoko, S. Zamir, P. Naumov and J. Bernstein, *J. Am. Chem. Soc.*, 2010, **132**, 14191–14202.
17 S. C. Sahoo, S. B. Sinha, M. S. Kiran, U. Ramamurty, A. F. Dericioglu, C. M. Reddy and P. Naumov, *J. Am. Chem. Soc.*, 2013, **135**, 13843–13850.
18 M. K. Panda, T. Runcevski, A. Husain, R. E. Dinnebier and P. Naumov, *J. Am. Chem. Soc.*, 2015, **137**, 1895–1902.
19 M. K. Panda, T. Runĉevski, S. C. Sahoo, A. A. Belik, N. K. Nath, R. E. Dinnebier and P. Naumov, *Nat. Commun.*, 2014, **5**, 4811.
20 E. Nauha, P. Naumov and M. Lusi, *CrystEngComm*, 2016, **18**, 4699–4703.
21 M. K. Panda, R. Centore, M. Causà, A. Tuzi, F. Borbone and P. Naumov, *Sci. Rep.*, 2016, **6**, 29610.
22 T. Takeda and T. Akutagawa, *Chem. – Eur. J.*, 2016, **22**, 7763–7770.
23 S. Ghosh, M. K. Mishra, S. Ganguly and G. R. Desiraju, *J. Am. Chem. Soc.*, 2015, **137**, 9912–9921.
24 S. C. Sahoo, M. K. Panda, N. K. Nath and P. Naumov, *J. Am. Chem. Soc.*, 2013, **135**, 12241–12251.
25 A. Khalil, E. Ahmed and P. Naumov, *Chem. Commun.*, 2017, **53**, 8470–8473.
26 A. Seeboth, D. Lötzsch, R. Ruhmann and O. Muehling, *Chem. Rev.*, 2014, **114**, 3037–3068.
27 J. H. Day, *Chem. Rev.*, 1963, **63**, 65–80.
28 M. A. White and M. LeBlanc, *J. Chem. Educ.*, 1999, **76**, 1201–1205.
29 Y. Xiong, Y. Ma, X. Yan, G. Yin and L. Chen, *RSC Adv.*, 2015, **5**, 53255–53258.
30 M. Avadanei, V. Cozan, S. Shova and J. A. Paixão, *Chem. Phys.*, 2014, **444**, 43–51.
31 H. Langhals and S. Kinzel, *Spectrochim. Acta, Part A*, 2011, **78**, 1212–1214.
32 P. Naumov, S. C. Lee, N. Ishizawa, Y. G. Jeong, I. H. Chung and S. Fukuzumi, *J. Phys. Chem. A*, 2009, **113**, 11354–11366.
33 M. Sliwa, A. Spangenberg, I. Malfant, P. G. Lacroix, R. Métivier, R. B. Pansu and K. Nakatani, *Chem. Mater.*, 2008, **20**, 4062–4068.
34 Y. Morita, S. Suzuki, K. Fukui, S. Nakazawa, H. Kitagawa, H. Kishida, H. Okamoto, A. Naito, A. Sekine, Y. Ohashi, M. Shiro, K. Sasaki, D. Shiomi, K. Sato, T. Takui and K. Nakasuji, *Nat. Mater.*, 2008, **7**, 48–51.
35 X. Yu, Y. Luo, W. Wu, Q. Yan, G. Zou and Q. Zhang, *Eur. Polym. J.*, 2008, **44**, 3015–3021.
36 A. Levy, S. Pogodin, S. Cohen and I. Agranat, *Eur. J. Org. Chem.*, 2007, **2007**, 5198–5211.
37 S. C. Lee, Y. G. Jeong, W. H. Jo, H.-J. Kim, J. Jang, K.-M. Park and I. H. Chung, *J. Mol. Struct.*, 2006, **825**, 70–78.
38 P. U. Biedermann, J. J. Stezowski and I. Agranat, *Chem. – Eur. J.*, 2006, **12**, 3345–3354.
39 H.-J. Suh, W.-T. Lim, J.-Z. Cui, H.-S. Lee, G.-H. Kim, N.-H. Heo and S.-H. Kim, *Dyes Pigm.*, 2003, **57**, 149–159.
40 E. Lambi, D. Gegiou and E. Hadjoudis, *J. Photochem. Photobiol., A*, 1995, **86**, 241–246.
41 J. F. D. Mills and S. C. Nyburg, *J. Chem. Soc.*, 1963, 308–321.
42 J. Troyano, O. Castillo, J. I. Martínez, V. Fernández-Moreira, Y. Ballesteros, D. Maspoch, F. Zamora and S. Delgado, *Adv. Funct. Mater.*, 2018, **28**, 1704040–1704051.
43 L. Zhai, W. W. Zhang, J. L. Zuo and X. M. Ren, *Dalton Trans.*, 2016, **45**, 3372–3379.
44 M. S. Denny and S. M. Cohen, *Angew. Chem.*, 2015, **127**, 9157–9160.
45 N. Guo and M. C. Leu, *Frontiers of Mechanical Engineering*, 2013, **8**, 215–243.
46 M. A. Luzuriaga, D. R. Berry, J. C. Reagan, R. A. Smaldone and J. J. Gassensmith, *Lab Chip*, 2018, **18**, 1223–1230.
47 G. A. Appuhamillage, J. C. Reagan, S. Khorsandi, J. R. Davidson, W. Voit and R. A. Smaldone, *Polym. Chem.*, 2017, **8**, 2087–2092.
48 J. R. Davidson, G. A. Appuhamillage, C. M. Thompson, W. Voit and R. A. Smaldone, *ACS Appl. Mater. Interfaces*, 2016, **8**, 16961–16966.
49 M. Dharmarwardana, R. P. Welch, S. Kwon, V. K. Nguyen, G. T. McCandless, M. A. Omary and J. J. Gassensmith, *Chem. Commun.*, 2017, **53**, 9890–9893.
50 M. A. Kobaisi, S. V. Bhosale, K. Latham, A. M. Raynor and S. V. Bhosale, *Chem. Rev.*, 2016, **116**, 11685–11796.
51 S. V. Bhosale, C. H. Jani and S. J. Langford, *Chem. Soc. Rev.*, 2008, **37**, 331–342.
52 S. Fomine, L. Fomina, R. Arreola and J. C. Alonso, *Polymer*, 1999, **40**, 2051–2058.
53 R. Rybakiewicz, I. Tszydel, J. Zapala, L. Skorka, D. Wamil, D. Djurado, J. Pecaut, J. Ulanski, M. Zagorska and A. Pron, *RSC Adv.*, 2014, **4**, 14089–14100.
54 J. Yin, K. Chaitanya and X.-H. Ju, *Can. J. Chem.*, 2015, **93**, 740–748.